ELSEVIER

Journal of Chromatography A, 721 (1996) 31–39

JOURNAL OF CHROMATOGRAPHY A

Performance of pH elution in high-performance affinity chromatography of proteins using non-porous silica

Wen-Chien Lee[a,*], Chien-Yi Chuang[b]

[a]*Department of Chemical Engineering, National Chung Cheng University, Chiayi, 621, Taiwan*
[b]*Department of Chemical Engineering, Chung Yuan Christian University, Chungli, 320, Taiwan*

First received 7 March 1995; revised manuscript received 4 July 1995; accepted 6 July 1995

Abstract

Non-porous silica with an average diameter of 1.4 μm was synthesized and derivatized for the high-performance affinity chromatography of proteins. The elution behaviour of proteins on a non-porous silica-based adsorbent was investigated both theoretically and experimentally using human immunoglobulin G (IgG) and immobilized protein A as the affinity pair. An equation used to predict the elution peak profiles was obtained. A comparison was also made between predicted and experimental elution peaks from chromatography of IgG on immobilized protein A. Experimental data indicated that samples with IgG contents up to 360 μg could be analysed chromatographically using a column packed with the non-porous silica-based affinity adsorbent. Alternation of the mobile phase pH is one of the conventional techniques employed to perform the elution of bound proteins from the column. Using this technique, the desorption rate constant and equilibrium association constant under elution conditions were found to have substantial effects on the elution time and the shape of the elution peak. The influence of sample load on the peak height was also examined.

1. Introduction

Non-porous adsorbents of small particle diameter have been employed for protein chromatography in recent years. These non-porous matrices are prepared from silica [1–9], agarose [10,11], poly(styrene–divinylbenzene) [12,13], TSK gel [14–17] and Bio-Rad MA7P (polymethacrylate coated with polyethyleneimine) [18–21]. Most of the adsorbents are used in the reversed-phase, ion-exchange and hydrophobic interaction chromatography of proteins. Cross-linked poly(styrene–divinylbenzene) microbeads have been surface coated with dinitrophenyl-amino acid for affinity chromatography of immunoglobulin E [22]. In a recent study [23], polystyrene microbeads were coated with poly(vinyl alcohol) and coupled with the reactive dye Cibacron Blue F3G-A for albumin adsorption. Among these non-porous matrices, only silica beads having an average size ranging from 1.5 to 2.1 μm were coupled with ligands via covalently binding to prepare affinity adsorbents [1–4]. In those investigations, using the immobilized ligands including triazine dyes and monoclonal antibody mouse immunoglobulin G (IgG), experimental breakthrough curves and adsorption isotherm of proteins on non-porous silica-based affinity matrices were determined in batch and frontal experiments. A mathematical model was

* Corresponding author.

0021-9673/96/$15.00
SSDI 0021-9673(95)00756-3

also proposed to predict the breakthrough curves from the affinity columns packed with non-porous particles [24]. For affinity chromatography operated in the HPLC mode [high-performance affinity chromatography (HPAC)], silica has advantages of good mechanical properties and hydrophilicity. In this work, protein A was immobilized on non-porous silica to provide an adsorbent for the HPAC of protein mixtures. The main objective was to study experimentally and theoretically the performance of HPAC employing non-porous silica beads, especially the behaviours of pH elution.

2. Experimental

2.1. Materials

Protein A from *Staphylococcus aureus* and human IgG (protein content 90% by mass; $E_{280}^{1\%} = 14$) were obtained from Sigma (St. Louis, MO, USA), amyl alcohol and glutaraldehyde (25% in water) from E. Merck (Germany), silicon tetrachloride (technical grade) from Reidel-de Haën (Seelze, Hannover, Germany) and γ-aminopropyltriethoxysilane from Aldrich (Milwaukee, WI, USA).

2.2. Preparation of non-porous silica-based adsorbents

Non-porous silica was made by following the procedure of Stober et al. [25] by reacting 16 ml of tetraamyl orthosilicate with 100 ml of an ammonia-saturated alcohol solution. The alcohol solution was prepared by passing ammonia through water–methanol–2-propanol (1:2:6). The synthesis reaction was carried out with stirring at 300 rpm for 24 h. The resulting silica was washed to neutrality with water and methanol, then dried in a vacuum oven at 150°C for 24 h. Tetraamyl orthosilicate was prepared by adding 120 ml of amyl alcohol dropwise to 25 ml of silicon tetrachloride in a 1-l flask with stirring and cooling in ice, followed by a 2-day reflux and fractionation. Modification of silica with 6% γ-aminopropyltriethoxysilane was carried out under anhydrous conditions [26]. The resulting aminopropylsilica was then activated with 5% glutaraldehyde in 0.05 *M* pyrophosphate buffer (pH 8.6) and shaken at room temperature for 12 h with protein A (1 mg/ml) in 0.1 *M* phosphate buffer (pH 7). The immobilized protein A was washed successively with phosphate buffer, 2 *M* NaCl and 0.1 *M* glycine.

2.3. HPAC procedure

Protein A–silica was slurry-packed into a 5.0 cm × 4.6 mm I.D. stainless-steel column using a column packer (Model CPP-085; Chemco). During the column packing, a 35-ml slurry reservoir containing 3 g of adsorbents was placed in front of the column to be packed. The buffer employed for column packing was phosphate buffer (pH 7). The HPAC equipment consists of a Gilson Model 305 high-pressure pump, a Gilson 115 UV detector and a sample injector with a 20-μl loop. The starting buffer for sample application and elution of non-retained components was 0.1 *M* potassium phosphate buffer (pH 7) prepared from K_2HPO_4 and KOH, whereas the retained components were eluted by stepwise changes to 0.1 *M* potassium phosphate buffer (pH 3) prepared from H_3PO_4 and KOH. The column was re-equilibrated with starting buffer for successive injections. Elution peaks of human IgG from the HPAC column were detected at 280 nm and integrated with a SIC Chromatocorder 12 integrator (System Instruments). The peak data were also collected via a PCL-812 A/D converter (Advantech) connected to a personal computer.

3. Theoretical

Affinity chromatography is a selective purification technique using high affinities between the bound ligand and the solutes (ligates) in the mobile phase. In a typical strong affinity chromatography, the equilibrium association constant for the affinity pair is extremely large. For the specific interaction between an antibody and an antigen, for example, association constants in the

range 10^7–10^8 M^{-1} are generally reported [27]. Protein A has very high affinity for the Fc region of immunoglobulins. The equilibrium association constant of Sephadex-immobilized protein A to rabbit IgG is reported to be $4.1 \cdot 10^8$ M^{-1} [28]. Therefore, for our system, the adsorption of desired proteins to an immobilized ligand is safely assumed to be irreversible. Owing to the high selectivity between the substances to be bound and the affinity matrix, all the components except for the one with specific interaction with the ligand would come out as a portion of the non-retained fraction. Elution of the bound protein can be achieved by reducing the association constant via alternation of the mobile phase pH and/or ionic strength [29]. Occasionally, the elution of an affinity-bound fraction can also be performed by applying a competitive inhibitor for the immobilized ligand to reduce the apparent association constant. The governing equations describing the concentrations of protein in the mobile phase (c) and on the adsorbent (q) during elution step can be expressed as follows:

$$\varepsilon \frac{\partial c}{\partial t} + (1-\varepsilon)\frac{\partial q}{\partial t} + u_0 \cdot \frac{\partial c}{\partial z} = 0 \tag{1}$$

$$\frac{\partial q}{\partial t} = k_a(q_m - q)c - k_d q \tag{2}$$

This model neglects axial dispersion effects and the influence of film resistance on the mass transfer rate. However, Eq. 2 is still useful in regarding the rate constants k_a and k_d as lumped parameters [30,31]. As the adsorption is irreversible, the column becomes saturated with the adsorbate only in the entrance end, provided that the sample loading is relatively smaller than the total binding capacity of the column. Let the starting point of elution be the beginning of the time-scale. The initial conditions are thus

$$t = 0, c = 0; q = \begin{cases} q_m, 0 < z < z_0 \\ 0, z_0 < z < L \end{cases} \tag{3}$$

where q_m is the maximum value of adsorbate concentration. The boundary condition is given by

$$z = 0, c = 0 \tag{4}$$

Eqs. 1–4 were solved analytically by following the method of Aris and Amundson [32] and the distribution describing the elution peak was obtained as

$$c(\tau, z = L) = \frac{\sqrt{k_0'/(\tau - 1)}}{K_e} \cdot \frac{I_1[2k_d^*\sqrt{k_0'(\tau-1)}][1 - e^{-k_0' k_d^* z_0'/L}]}{I_0[2k_d^*\sqrt{k_0'(\tau-1)}] + \Phi[k_d^*(\tau-1), k_0' k_d^*] + e^{-k_0' k_d^* z_0'/L}\Phi[k_0' k_d^*, k_d^*(\tau-1)]} \tag{5}$$

The function Φ is defined as

$$\Phi(u, v) = e^u \int_0^u e^{-s} I_0(2\sqrt{vs})\, ds \tag{6}$$

In Eq. 5, K_e ($= k_a/k_d$) is the association constant under the elution conditions and $k_0' = (1-\varepsilon)q_m K_e/\varepsilon$ is the limiting capacity factor, i.e., the capacity factor at zero sample concentration. The non-dimensional variable and parameter in Eq. 5 are defined as $\tau = tu_0/\varepsilon L$ and $k_d^* = k_d \varepsilon L/u_0$. Eq. 5 describes simply the dependence of the peak profiles (the effluent concentration varying with non-dimensional time τ) on the loading factor defined by z_0/L and two additional parameters, K_e and k_d^*. This loading factor equals the ratio of the amount of solute ($w_x = u_0 A_c c_0 t_{inj}$) injected to the saturation capacity of the column [$w_s = (1-\varepsilon)A_c L q_m$]. If the column is made by following a constant procedure and operated under given analysis conditions, all the parameters ε, u_0, A_c, L, c_0 and t_{inj} are known, except for K_e and k_d^*. Therefore, only two parameters, K_e and k_d^*, control the elution peak profiles. The first parameter is a thermodynamic variable that can be adjusted by changing the mobile phase pH and/or ionic strength, whereas the latter is a dimensionless desorption rate constant and subject to be evaluated from experimental results.

4. Results and discussion

4.1. Preparation of non-porous silica-based affinity adsorbent

Synthesis of non-porous, monodispersed silica beads was achieved by the use of tetraamyl

orthosilicate and an ammonia-saturated alcohol solution. The prepared non-porous silica was determined to have an average diameter of 1.4 μm and a surface area of 5.1 m^2/g calculated with the BET equation using nitrogen as the adsorbate. A comparison of Fourier transform IR spectrum of the non-porous silica with that of a commercial porous silica (Wakogel C-200) revealed that the two kinds of silica are identical in their composition. The particle size distribution of the prepared silica is shown in Fig. 1. This distribution, although covering two orders of magnitude, is monodispersed. The growth of silica beads was controlled by the concentration of ammonia, the composition of alcohol solution, the kind of tetraakyl orthosilicate used and the reaction time. The use of tetraamyl orthosilicate under constant experimental conditions caused a larger particle size than that with tetraethyl orthosilicate. The higher the concentration of ammonia employed, the larger was the average particle size. Accordingly, the largest spheres were obtained when the reaction mixture was saturated with ammonia. Fig. 2 shows the 2- and 24-h growth of silica beads from the controlled hydrolysis of tetraamyl orthosilicate in ammonia-saturated alcohol solution. Immunoaffinity adsorbents were obtained from the aminopropylsilica activated with glutaraldehyde and then coupled with protein A. The column (5 cm × 0.46 cm I.D.) packed with immobilized protein A was operated in the HPLC mode at a flow-rate of 1.5 ml/min against a pressure gradient of 300 bar. This column pressure was higher owing to the use of fine particles.

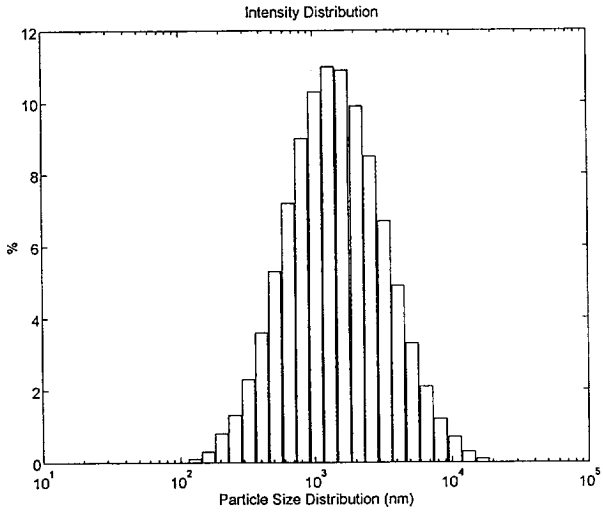

Fig. 1. Particle size distribution of the prepared non-porous silica beads.

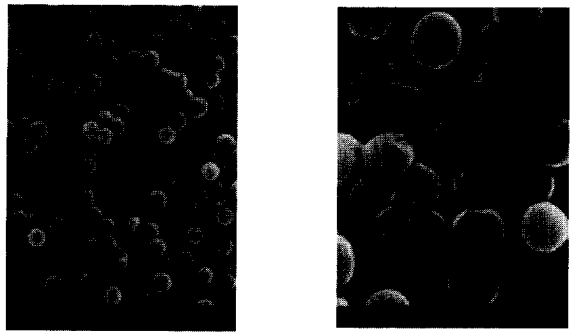

Fig. 2. Growth of silica beads from the controlled hydrolysis of tetraamyl orthosilicate in ammonia-saturated alcohol solution: (a) 2 and (b) 24 h growth.

4.2. Chromatogram of IgG on immobilized protein A

When pure human IgG was applied to the high-performance affinity column, only a minute amount of protein was not retained by the column. The retained proteins could be eluted by stepwise changes to the pH 3 buffer as shown in Fig. 3. The non-retained fractions were eluted in 0.42 min, while the retained proteins were eluted in ca. 6 min following the stepwise change of buffer from 0.1 *M* potassium phosphate (pH 7) to 0.1 *M* potassium phosphate (pH 3). This retention time for the non-retained peak indicates a total dead volume of 0.63 ml, which includes the extra-column dead volume of 0.31 ml. Calibration graphs could be established either from the elution peak height or peak area vs. IgG concentration. Fig. 4 shows that when 9-μl samples of IgG in a concentration ranging

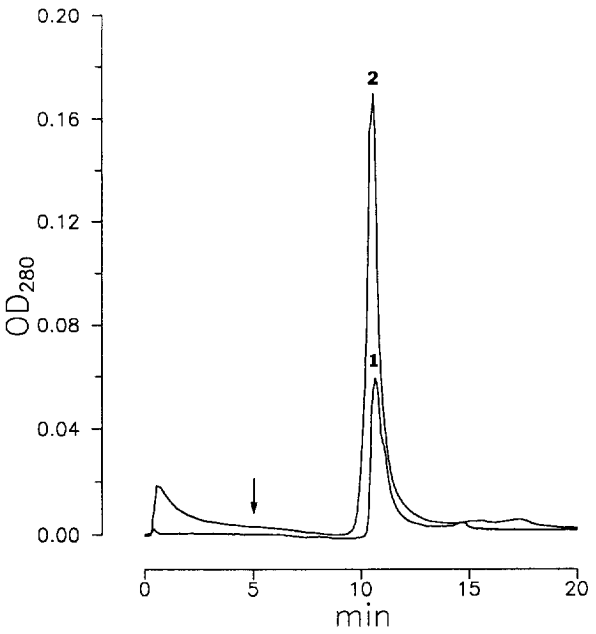

Fig. 3. Chromatograms of human IgG on an HPAC column (5 cm × 0.46 cm I.D.) packed with immobilized protein A on non-porous silica. The arrows indicate stepwise changes in mobiles phase from pH 7 to 3. Flow-rate, 1.5 ml/min; sample volume, 9 μl. Sample concentration: 1 = 15; 2 = 40 g/l.

from 2.5 to 40 mg/ml were prepared as the standards, straight lines were obtained from the plots of peak area vs. IgG concentration and also peak height vs. IgG concentration. The data indicate that samples with IgG contents up to ca. 360 μg could be analysed chromatographically.

The retention time for the non-retained portion of proteins did not change with a sample load up to 180 μg (Fig. 5). However, a significant proportion of the proteins was eluted in the non-retained fraction when the sample load exceeded 180 μg. This elution suggests that a split peak could occur at this overloading level of sample application, as evidenced by peak 2 in Fig. 3. The non-retained peak in the IgG chromatogram constituted less than 3% of the total absorbance of the sample whenever the sample contained an amount of IgG less than 180 μg. This minor fraction was probably IgG 3, which does not carry any affinity for protein A and passed unretarded through the column. However, the non-retained peak may be partially due to the so called "split-peak" effect. It has been reported [33] that split peaks occur even in linear chromatography, i.e., when the sample size is extremely small.

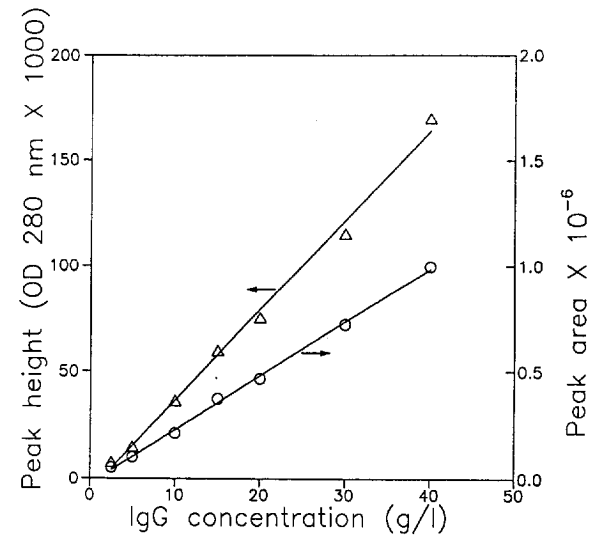

Fig. 4. Calibration graphs of peak height (peak area) vs. IgG concentration in 9-μl samples. Chromatographic conditions as in Fig. 3.

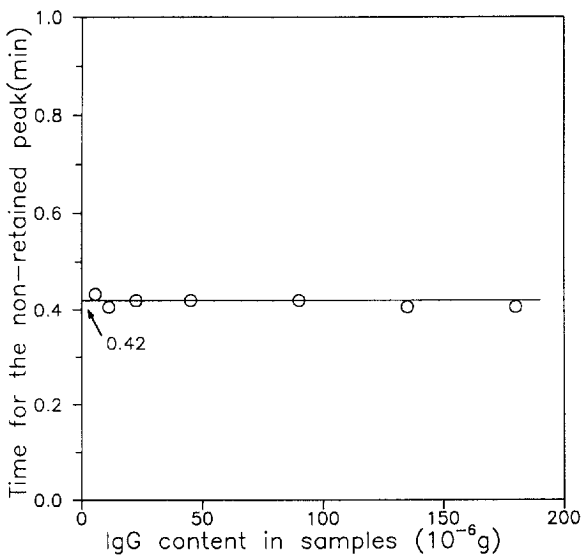

Fig. 5. Variation of the retention time for non-retained peaks with sample loading.

4.3. Predicting the behaviour of pH elution

The elution profile could be predicted by Eq. 5, provided that the amount of solute loaded into the column was insignificant compared with the column capacity. In the affinity chromatographic system presented in this work, operational parameters were determined as $\varepsilon = 0.39$, $u_0 = 9$ cm/min (which corresponds to a flow-rate of 1.5 ml/min) and $L = 5$ cm. The extrapolation of the retention time for the eluted peak to zero sample load is 6.04 min (Fig. 6). The limiting capacity factor is thus calculated as $k'_0 = [(6.04 \cdot 1.5) - 0.32]/0.32 = 27.3$, where 0.32 (ml) is the column void volume. Taking $k^*_d = 20$ and $K_e = 0.5$ l/g, the predicted elution profiles using Eq. 5 are shown in Fig. 7, in which 5.21 min was added to the elapsed time (5 min before the starting-point of elution and 0.21 min for the time required to flow through the extra-column dead volume). Corresponding elution curves resulting from experiments are also shown in Fig. 7. The correlation of the O.D. at 280 nm with the protein concentration, 1 g/l $\approx$ 0.57 O.D., was obtained by plotting the elution peak area versus the sample load over the range of small sample sizes.

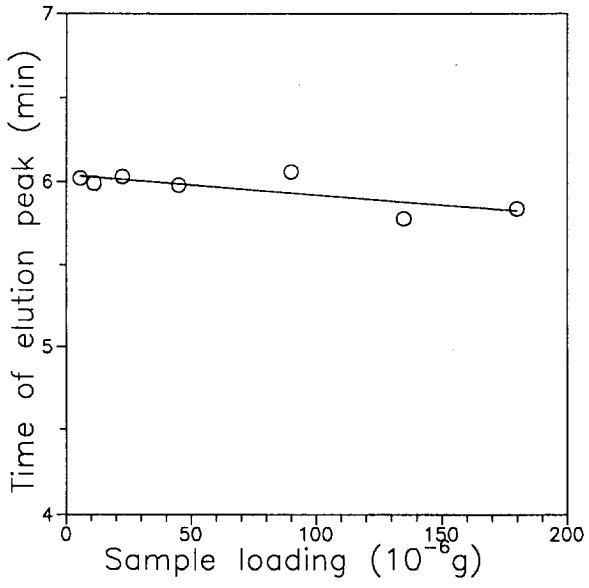

Fig. 6. Variation of the retention time for retained peaks with sample loading.

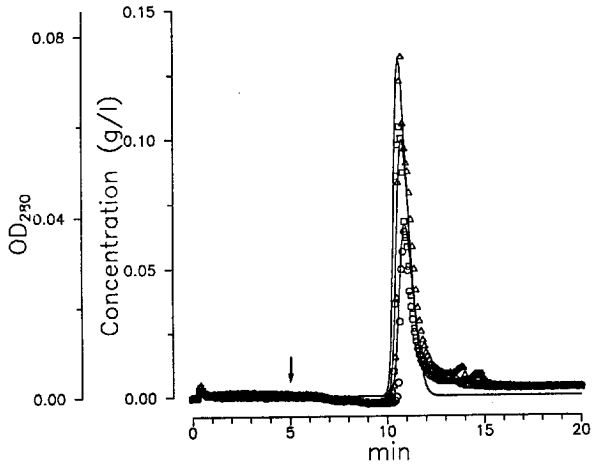

Fig. 7. Predicted (solid lines) and experimental (data points) elution profiles for high-performance affinity chromatography of IgG on immobilized protein A. Experimental conditions as in Fig. 3, except sample concentration: △ = 20; □ = 15; ○ = 10 g/l. Parameter values for the predicted case are $k'_0 = 27.3$, $k^*_d = 20$ and $K_e = 0.5$ l/g.

The k^*_d and K_e values were determined by matching the experimental data with the predictions of the elution peak described by Eq. 5. A slight shift occurred in the baseline after the elution, thereby making an excellent fit to the whole elution peaks nearly impossible. The influences of sample concentration (injection volume 9 μl) on the peak height and peak shape are similar in both the predicted and experimental data, as indicated in Fig. 7.

The maximum binding capacity was calculated from k'_0 and K_e for this affinity system as $q_m = 34.9$ g/l. The rate constants of adsorption and desorption could be calculated as $k_a = 0.77$ l g^{-1} s^{-1} ($=1.2 \cdot 10^5$ M^{-1} s^{-1}) and $k_d = 1.5$ s^{-1}, respectively, using $k^*_d = 20$ and $K_e = 0.5$ l/g ($=7.8 \cdot 10^4$ M^{-1}). The k_a value is close to that for adsorption of lysozyme on Cibacron Blue F3GA with non-porous silica (1.5 μm), which falls in the range 0.375–1.753 l g^{-1} s^{-1}. The k_a might not take into account the effect of film resistance, since a higher flow-rate (1.5 ml/min) was used in this work. The sharper peaks appearing in Fig. 7 imply a higher desorption rate and mass transfer rate, which is attributed to a larger film

mass-transfer coefficient. An increase in k_d tends to sharpen the elution peak and increase the peak height.

As the column was packed with a fixed amount of affinity adsorbents with a known binding capacity, the factors having an effect on the shape and height of the elution peaks according to Eq. 5 are flow velocity u_0, sample size w_x (or z_0), desorption rate constant k_d and association constant K_e under the elution conditions. An increase in flow velocity causing a reduction in the elution time is obvious from the definition of the non-dimensional time $\tau = tu_0/\varepsilon L$. Both the predicted peak area and peak height definitely increase with increasing sample load, as shown in Fig. 7. The predicted peak heights varying with sample concentration (injection volume 9 μl) for several k_d^* values are shown in Fig. 8. Straight lines passing through the origin were obtained from the plots of peak height vs. sample load for lower values of k_d^*. Interestingly, the loci of the peak height become slightly curvilinear over the same range of sample load as k_d^* increases to 20. This is because the peak becomes more asymmetric as k_d^* increases. The calibration graph for HPAC based on peak height is much simpler than that on the peak area.

The large value of k_d indicates a rapid desorption rate of the bound compounds from the adsorbent. Fig. 9 shows that when the rate constant becomes larger, the elution peak becomes sharper and the time required to elute all bound proteins becomes shorter because of the faster rate. The peak height increases with the rate constant owing to the sharper peak and constant value of the peak area. The rate constant is generally dependent on mobile phase composition and pH. If the effect of film resistance becomes significant and must be taken into account, the rate constant in this case is an apparent value and a weak function of the flow-rate. A higher flow-rate enhances the mass transfer, i.e., the film mass-transfer resistance is reduced. The film mass-transfer coefficient can be estimated from a J factor correlation proposed by Wilson and Geankoplis [34]. This correlation (Eq. 7) is valid for liquid with a Reynolds number ($Re \equiv d_p u_0/\nu$) range of

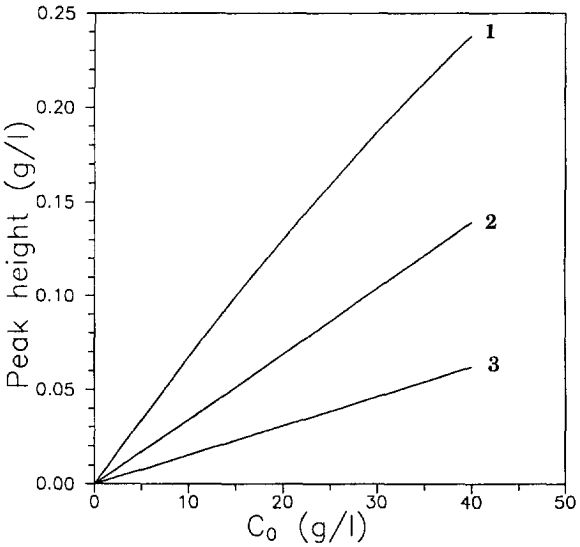

Fig. 8. Plots of peak height vs. solute concentration in 9-μl samples for k_d^* = (1) 20, (2) 5 and (3) 1. Parameters for the prediction are $d_p = 1.4 \cdot 10^{-4}$ cm^2, $u_0 = 0.15$ cm/s, $L = 5$ cm, $\varepsilon = 0.39$, $K_e = 0.5$ l/g and $q_m = 34.9$ g/l ($k_0' = 27.3$).

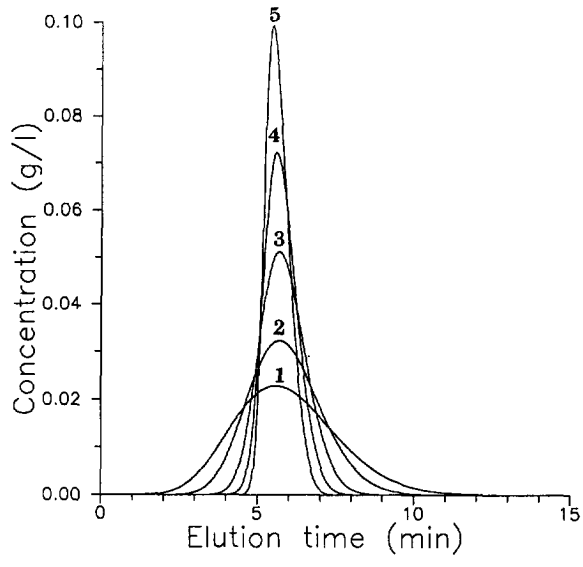

Fig. 9. Influence of rate constant on the profile of the elution peak. Parameters for the prediction are $K_e = 0.5$ l/g, q_m = 34.9 g/l and $C_0 = 15$ g/l; others as in Fig. 8. The non-dimensional rate constant k_d^* = (1) 1, (2) 2, (3) 5, (4) 10 and (5) 20.

0.0016–55 and a Schmidt number ($Sc \equiv \nu/D_m$) range of 165–70 600.

$$J \equiv \frac{k_f}{u_0}\left(\frac{\nu}{D_m}\right)^{2/3} = \frac{1.09}{\varepsilon}\left(\frac{d_p u_0}{\nu}\right)^{-2/3} \quad (7)$$

Taking the experimental value of the molecular diffusivity for IgG (M_r 156 000) [35], $4.0 \cdot 10^{-7}$ cm^2/s, and $\nu = 1 \cdot 10^{-2}$ cm^2/s (dilute aqueous solution at 293 K), k_f can be calculated using Eq. 7 to be $3 \cdot 10^{-2}$ cm/s. This k_f value is close to that reported by Mao et al. [24], $3.5 \cdot 10^{-2}$ cm/s, for 1.5-μm non-porous particles. A comparison is next made of the contribution of film mass-transfer coefficient with that of the desorption rate constant to the peak spreading in the range of linear chromatography (zero sample size):

$$\frac{1}{k_d} = 0.67\ s >> \frac{\varepsilon d_p k_0'}{6(1-\varepsilon)} \cdot \frac{1}{k_f} = 0.014\ s$$

On the basis of that comparison, we can conclude that the elution process is desorption-dominating and the assumption of neglecting film resistance is acceptable.

Increasing K_e significantly delays the appearance of the elution peak, as shown in Fig. 10. A small K_e indicates a weak binding affinity between the protein and the immobilized ligand. Thus, the smaller is K_e, the much easier is bound protein elution. The results in Fig. 10 indicate that the mean retention time and the time required to conclude the elution become shorter because of weaker binding. The equilibrium association constant K_e, which is a thermodynamic property, depends on the pH, ionic strength and composition of the mobile phase at the elution stage. Therefore, the optimum approach to reduce the analytical time is to select elution conditions making the K_e value as small as possible. Alteration of the pH of the mobile phase is one of the most common and simplest ways to reduce the K_e value. The dependence of pH on the variation of K_e is easily obtained experimentally [29,36]. As the relationship between pH and binding constant is known, the elution peak can be predicted. In the IgG–protein A system presented, the association constant was lowered to $7.8 \cdot 10^4$ M^{-1} by changing the buffer pH from 7 to 3. This value of the association constant during elution falls in the range of $1.5 \cdot 10^4$–$1.2 \cdot 10^6$ M^{-1}, as suggested by Antonsen et al. [29]. To give a faster elution, K_e should be reduced as much as possible. Usually the association constant and then the elution time can be reduced considerably by using strong elution conditions, e.g., extremely low pH. However, retaining the activity of product and ligand and the binding capacity of the column is sometimes the determining factor in selecting the elution conditions. The column should retain its binding capacity and, in particular, the protein ligand should not be irreversibly damaged.

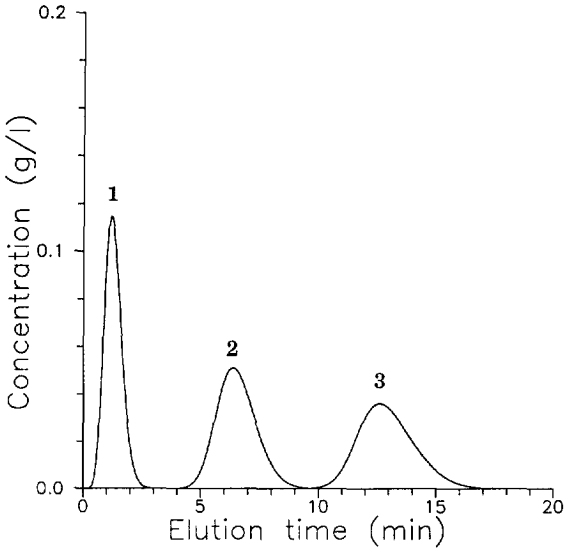

Fig. 10. Influence of association constant on the elution peak profile. Parameters for the prediction are $k_d^* = 5$, $q_m = 34.9$ g/l and $C_0 = 15$ g/l; others as in Fig. 8. The association constant K_e = (1) 0.1, (2) 0.5 and (3) 1 l/g.

Symbols

A_c cross-sectional area of the empty column, cm^2
c concentration of solute in mobile phase, g l^{-1}
c_0 sample concentration, g l^{-1}
D_m molecular diffusivity of solute, cm^2 s^{-1}
d_p diameter of adsorbent particle, cm
k_0' capacity factor at zero sample concentration

k_a adsorption rate constant at elution stage, l g^{-1} s^{-1} or M^{-1} s^{-1}
k_d desorption rate constant at elution stage, s^{-1}
k_f film mass-transfer coefficient, cm s^{-1}
k_d^* non-dimensional desorption rate constant
K_e association constant at elution stage = k_a/k_d, l g^{-1} or M^{-1}
L length of the column, cm
q sorbate concentration, g l^{-1}
q_m maximum sorbate concentration, g l^{-1}
t time, s
t_{inj} time interval of sample injection, s
u_0 superficial velocity, cm s^{-1}
z linear coordinate along the column, cm
z_0 length of the column saturated with adsorbate, cm

Greek letters

ε void fraction of the packed column
τ non-dimensional time
ν dynamic viscosity, cm^2 s^{-1}

Acknowledgement

This study was supported by the National Science Council of the Republic of China under contract NSC 82-0402-E033-046.

References

[1] B. Anspach, K.K. Unger, J. Davies and M.T.W. Hearn, J. Chromatogr., 475 (1988) 195.
[2] A.I. Liapis, B. Anspach, M.E. Findley, J. Davies, M.T.W. Hearn and K.K. Unger, Biotechnol. Bioeng., 34 (1989) 467.
[3] F.B. Anspach, A. Johnston, H.J. Wirth, K.K. Unger and M.T.W. Hearn, J. Chromatogr., 499 (1990) 103.
[4] H.J. Wirth, K.K. Unger and M.T.W. Hearn, J. Chromatogr., 550 (1990) 383.
[5] K.K. Unger and G. Jilge, J. Chromatogr., 359 (1986) 61.
[6] G. Jilge, R. Janzen, H. Giesche and K.K. Unger, J. Chromatogr., 397 (1987) 71.
[7] R. Janzen, K.K. Unger and H. Giesche, J. Chromatogr., 397 (1987) 81.
[8] R. Janzen, K.K. Unger and H. Giesche, J. Chromatogr., 397 (1987) 91.
[9] K. Kalghatgi and C. Horvath, J. Chromatogr., 398 (1987) 335.
[10] S. Hjerten and J.L. Liao, J. Chromatogr., 457 (1988) 165.
[11] J.L. Liao and S. Hjerten, J. Chromatogr., 457 (1988) 175.
[12] Y.-F. Maa and C. Horvath, J. Chromatogr., 445 (1988) 71.
[13] M.A. Rounds and F.E. Regnier, J. Chromatogr., 443 (1988) 73.
[14] Y. Kato, T. Kitamura, A. Mitsui and T. Hashimoto, J. Chromatogr., 398 (1987) 327.
[15] Y. Kato, T. Kitamura, A. Mitsui and T. Hashimoto, J. Chromatogr., 483 (1989) 401.
[16] Y. Kato, S. Nakatani, T. Kitamura, A. Mitsui and T. Hashimoto, J. Chromatogr., 502 (1990) 422.
[17] Y. Kato, Y. Yamasaki, A. Onaka, T. Kitamura and T. Hashimoto, J. Chromatogr., 478 (1989) 264.
[18] D.J. Burke, J.K. Duncan, L.C. Dunn, L. Cummings, C.J. Siebert and G.S. Ott, J. Chromatogr., 353 (1986) 425.
[19] D.J. Burke, J.K. Duncan, C.J. Siebert and G.S. Ott, J. Chromatogr., 359 (1986) 533.
[20] I. Mazsaroff, M.A. Rounds and F.E. Regnier, J. Chromatogr., 411 (1987) 452.
[21] J.K. Duncan, A.J.C. Chen and C.J. Siebert, J. Chromatogr., 397 (1987) 3.
[22] S. Wongyai, J.M. Varga and G.K. Bonn, J. Chromatogr., 536 (1991) 155.
[23] A. Tuncel, A. Denizli, D. Purvis, C.R. Lowe and E. Piskin, J. Chromatogr., 634 (1993) 161.
[24] Q.M. Mao, A. Johnston, I.G. Prince and M.T.W. Hearn, J. Chromatogr., 548 (1991) 147.
[25] W. Stober, A. Fink and E. Bohn, J. Colloid Interface Sci., 26 (1968) 62.
[26] R.-M. Chang and W.-C. Lee, J. Chem. Technol. Biotechnol., 59 (1994) 133.
[27] M.L. Yarmush, A.H. Weiss, K.P. Antosen, D.J. Odde and D.M. Yarmush, Biotechnol. Adv., 10 (1992) 413.
[28] R. Lindmark, C. Biriell and J. Scand, J. Immunol., 14 (1981) 409.
[29] K.P. Antonsen, C.K. Colton and M.L. Yarmush, Biotechnol. Prog., 7 (1991) 159.
[30] F.H. Arnold and H.W. Blanch, J. Chromatogr., 355 (1986) 13.
[31] J.L. Wade, A.F. Bergold and P.W. Carr, Anal. Chem., 59 (1987) 1286.
[32] R. Aris and N.R. Amundson, Mathematical Methods in Chemical Engineering, Prentice-Hall, Englewood Cliffs, NJ, 1973.
[33] D.S. Hage, R.R. Walters and H.W. Hethcote, Anal. Chem., 58 (1986) 274.
[34] E.J. Wilson and C.J. Geankoplis, Ind. Eng. Chem. Fundam., 5 (1966) 9.
[35] M.T. Tyn and T.W. Gusek, Biotechnol. Bioeng., 35 (1990) 327.
[36] K.A. Kang and D.D. Ryu, Biotechnol. Prog., 7 (1991) 205.